Korean J. Chem. Eng., 32(1), 51-61 (2015)
DOI: 10.1007/s11814-014-0195-z

pISSN: 0256-1115
eISSN: 1975-7220

Development of the Al_2O_3-supported $NaNO_3$-$Na_2Mg(CO_3)_2$ sorbent for CO_2 capture with facilitated sorption kinetics at intermediate temperatures

Hwimin Seo*, Da Young Min*, Na Young Kang*, Won Choon Choi*, Sunyoung Park*, Yong-Ki Park*, and Deuk Ki Lee,†**

*Green Chemistry Process Research Division, Korea Research Institute of Chemical Technology, Daejeon 305-600, Korea
**Department of Fire Safety, Gwangju University, Gwangju 503-703, Korea
(*Received 7 March 2014 • accepted 9 July 2014*)

Abstract−For the development of a dry solid sorbent having quite fast CO_2 sorption kinetics in an intermediate temperature range of 245-300 °C to be applicable to a riser-type fluidized bed carbonator, samples of Al_2O_3-supported $MgCO_3$ (1.2 mmol/g) promoted with different molar amounts of Na_2CO_3 (1.2, 1.8 mmol/g) and/or $NaNO_3$ (0.6 mmol/g) were prepared by incipient wetness pore volume impregnation. For a reference, an unsupported bulk phase sorbent of $NaNO_3$-$Na_2Mg(CO_3)_2$ was also prepared. From the sorption reaction using a gas mixture containing CO_2 by 2.5-10% at 1 bar for the sorbents after their activation to MgO, Al_2O_3-supported sorbents were featured by their rapid carbonation kinetics in contrast to the unsupported sorbent showing a quite slow carbonation behavior. The addition of Na_2CO_3 to the $MgCO_3/Al_2O_3$ sorbent made MgO species more reactive for the carbonation, bringing about a markedly enhanced kinetic rate and conversion, as compared with the unpromoted $MgCO_3/Al_2O_3$ sorbent having a small negligible reactivity. The addition of $NaNO_3$ to $MgCO_3/Al_2O_3$ or to Na_2CO_3-$MgCO_3/Al_2O_3$ induced the same promotional effects, but to a lesser magnitude, as observed for the Na_2CO_3 addition. It was also characteristic for all these $MgCO_3$-based sorbents that initial carbonation conversions with time appeared as sigmoid curves. For the Al_2O_3-supported sorbent comprised of $NaNO_3$, Na_2CO_3, and $MgCO_3$ by 0.6, 1.8, and 1.2 mmols, respectively, per gram sorbent, showing the best kinetic performance, a kinetic equation capable of reflecting such sigmoid conversion behavior was established, and its applicability to a riser carbonator was examined throughout a simple model calculation based on the kinetics obtained.

Keywords: CO_2 Capture, Supported Sorbent, Magnesium Carbonate, Sodium Carbonate, Kinetics

INTRODUCTION

With growing worldwide concern about global warming, various research efforts have been made toward the development of more efficient technologies to capture CO_2 from such large point sources as coal-fired power stations. Though a variety of CO_2 capture technologies have been proposed, post-combustion CO_2 capture from the flue gas is regarded as one of the key technology options to reduce the amount of the atmospheric emission, because this can be potentially retrofitted to the existing fleet of coal-fired power stations [1,2]. Recently, a dry CO_2 capture process using solid sorbents like Na_2CO_3 or K_2CO_3 received much attention as an alternative to the conventional absorption processes using alkaline solvents with such inherent drawbacks as high equipment corrosion rate, high energy consumption in regeneration, and a large absorber volume required [3-5]. However, even the dry sorbent process is still far from its full commercial operation because of its low process efficiency, mainly attributed to the high energy requirement in the regenerative decarbonation of carbonated sorbents.

To increase the energy efficiency of a dry sorbent process, researchers at Korea Research Institute of Chemical Technology (KRICT) recently proposed a new CO_2 capture process consisting of three - low, intermediate, and high - temperatures-staged sorption/regeneration cycles, of which the main idea is to make use of the heat evolved in the sorption reaction at higher temperature stage as the thermal energy required for the sorbent regeneration at lower temperature stage through the cascaded inter-stage heat integration. As described by Kim et al. [6], each stage of the process is composed of a sorption/regeneration cycle using a couple of separate fluidized bed reactors, through which sorbent particles circulate to be carbonated/decarbonated. From the simulation analysis for the three-stage process adopting the sorbents (sorption/regeneration temperatures) of K_2CO_3 (50/170 °C), MgO (270/450 °C), and Li_4SiO_4 (550/750 °C) for the low, intermediate, and high temperature stages, respectively, Kim et al. [6] estimated that the total energy demand per ton of CO_2 recovery with the three stages could be reduced to 1.73-1.91 MJ/kg-CO_2. This is much lower than the recently reported energy consumption of 2.44-2.53 MJ/kg-CO_2 for a solvent absorption process by Mitsubishi Heavy Industry [7]. Although the fluidized bed of the dense (bubbling) type or the dilute (fast) type could be employed for sorption/regeneration reactors of this multi-staged process, a dilute fast bed known as a riser or a circulating fluidized bed would be the choice of priority, considering its high throughput in the handling capacity of the flue gas, simple structure favorable for easy

†To whom correspondence should be addressed.
E-mail: dklee@gwangju.ac.kr

scale-up, and properties of excellent heat and mass transfer. In view of the short contact time between the sorbent particles and the flue gas inside the riser, the most important requirement of a solid sorbent for its application to the riser sorber/regenerator would be its kinetic swiftness in the carbonation/decarbonation reactions. The adoption of a riser reactor as a carbonator for a low temperature stage CO_2 capture was demonstrated for a sorbent based on K_2CO_3 [8] or Na_2CO_3 [9], or for a supported amine sorbent [10]. Such an application of a riser carbonator to this low temperature stage CO_2 capture would be possible due to the fast carbonation kinetics of the sorbent, as described by a kinetic equation for K_2CO_3/ZrO_2 [11] or silica-immobilized amine [12].

The present study aims at the development of an intermediate temperature sorbent with quite fast carbonation kinetics, enough to be applicable to the riser sorber of the intermediate stage. The sorbent developed here is based on the Na_2CO_3-promoted $MgCO_3$. Zhang et al. [13] proposed that CO_2 sorption proceeds through the reversible formation of Na-Mg double salt following reaction (1):

$$MgO+Na_2CO_3+CO_2(g)\leftrightarrow Na_2Mg(CO_3)_2 \quad (1)$$

They [13] synthesized the bulk phase sorbent of double salt, $Na_2Mg(CO_3)_2$, through such a wet-chemistry route via precipitation and filtration using water-soluble metal salts as described by Mayorga et al. [14] From the multi-cycle tests of CO_2 sorption/desorption in 100% CO_2 at 380/470 °C, they [13] reported that the double salt sorbent had a very high CO_2 capture capacity of 3.4 mmol CO_2/g, as compared to the unmodified MgO of 0.24 mmol/g at 200 °C. They [13] indicated that the amount of retained Na_2CO_3 in the initial synthesis step directly affected the performance, and that the impurity phase in the bulk synthesized sorbent, $NaNO_3$, was identified as a key component in facilitating CO_2 sorption by the Na-Mg double salt. However, for the wet-chemistry route synthesis of the bulk $NaNO_3$-$Na_2Mg(CO_3)_2$, the amounts of Na_2CO_3 and $NaNO_3$ retained in the resultant filter cake were reported [13] to be difficult to control because of their high water solubility. As a candidate of the sorbent for the intermediate stage in the proposed 3-staged CO_2 capture process, $NaNO_3$-$Na_2Mg(CO_3)_2$ as described above is promising for its high CO_2 uptake capacity and its intermediate sorption temperature once the problem in the reproducibility of its synthesis technique has been solved. And, for its application to the riser sorber, the $NaNO_3$-$Na_2Mg(CO_3)_2$ sorbent is required to have quite fast reaction kinetics, but, no kinetic information is available up to now.

In the present study, we try to synthesize the sorbent of $NaNO_3$-$Na_2Mg(CO_3)_2$ supported on porous Al_2O_3 beads using the technique of pore volume impregnation at incipient wetness. With this technique, controlled amounts of $MgCO_3$, Na_2CO_3 and $NaNO_3$ are retainable inside pores of a support. To obtain the sorption reaction rate data, samples of Al_2O_3-supported $MgCO_3$ (1.2 mmol/g) promoted with different molar amounts of Na_2CO_3 (1.2, 1.8 mmol/g) and/or $NaNO_3$ (0.6 mmol/g) were prepared by such an impregnation technique, and tested using a gas mixture containing CO_2 by 2.5-10% at 1 bar. For the Al_2O_3-supported sorbent of $NaNO_3$-$Na_2Mg(CO_3)_2$ showing the best kinetic performance, a kinetic equation was derived, and its applicability to a riser sorber was evaluated on the basis of the kinetics obtained.

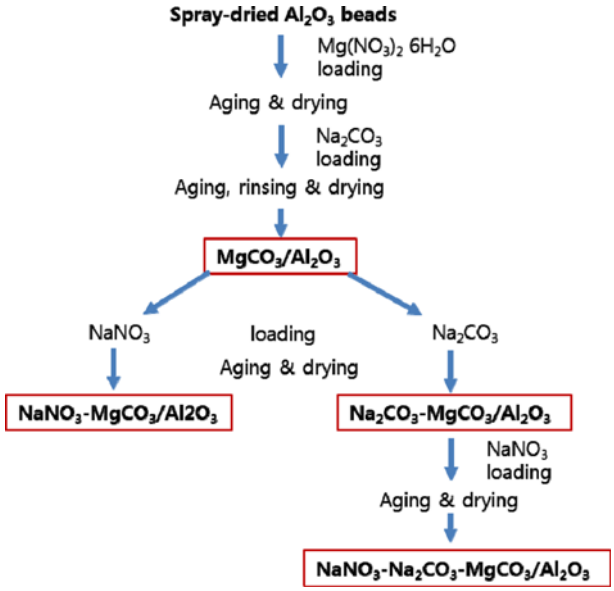

Fig. 1. Procedure for the preparation of Al_2O_3-supported $MgCO_3$-based sorbents (Aging at room temperature for 12 h, and drying at 120 °C for 12 h).

EXPERIMENTAL

1. Sorbent Preparation

Spherical beads of Al_2O_3 of 100 μm size were prepared by spray drying method. After calcination at 550 °C for 6 h, Al_2O_3 beads (BET surface area, 216 m^2/g; pore volume, 0.4 cm^3/g) were used for the sorbent support. Fig. 1 shows the preparation procedure for Al_2O_3-supported $MgCO_3$-based sorbents. Loading of $MgCO_3$ onto Al_2O_3 was achieved by successive two-step impregnations as follows: First, Al_2O_3 beads were pore-filled by incipient wetness using aqueous solution of $Mg(NO_3)_2{\cdot}6H_2O$ (98%, Samchun). The impregnated sample was aged at room temperature for 12 h, and then oven-dried at 120 °C for 12 h. The second step was to precipitate Mg^{2+} ions remaining inside the support pores into $MgCO_3$. As a carbonate precipitant for this, saturated aqueous solution of Na_2CO_3 (99%, Samchun) was pore-filled to the $Mg(NO_3)_2$-loaded Al_2O_3 by incipient wetness. After aging for 12 h, the sample was gently washed using deionized water to remove the pore-remaining water-soluble salts, and oven-dried to obtain the $MgCO_3/Al_2O_3$ sorbent containing Mg by 1.2 mmol/g (10 wt% as $MgCO_3$, or 5 w% as MgO after the calcination for activation). Other $NaNO_3$ (99.5%, Samchun) and/or Na_2CO_3-promoted Al_2O_3-supported sorbents were prepared by incipient wetness impregnation of each salt-dissolved solution onto the $MgCO_3/Al_2O_3$ following the procedure shown in Fig. 1. These Al_2O_3-supported samples were activated by the calcination in a muffle furnace at 450 °C for 4 h in air for the CO_2 sorption reaction test. Table 1 summarizes the Al_2O_3-supported $MgCO_3$-based sorbents prepared. BET surface area and pore volume of the sample SN(0.6)SC(1.8)MC(1.2) were 120 m^2/g and 0.28 cm^3/g, respectively.

Along with these supported sorbents, an unsupported bulk phase double salt-sorbent of $NaNO_3$-$Na_2Mg(CO_3)_2$ was prepared, refer-

Table 1. Al_2O_3-supported $MgCO_3$-based sorbents prepared

Sorbent notation[a]	Salt amounts, mmol/g			Composition, wt%			
	$NaNO_3$	Na_2CO_3	$MgCO_3$	$NaNO_3$	Na_2CO_3	MgO	Al_2O_3
SN(0)SC(0)MC(1.2)	0	0	1.2	0	0	5.0	95.0
SN(0)SC(1.2)MC(1.2)	0	1.2	1.2	0	11.7	4.5	83.8
SN(0)SC(1.8)MC(1.2)	0	1.8	1.2	0	16.6	4.2	79.2
SN(0.6)SC(0)MC(1.2)	0.6	0	1.2	5.1	0	4.8	90.1
SN(0.6)SC(1.2)MC(1.2)	0.6	1.2	1.2	4.5	11.2	4.3	80.1
SN(0.6)SC(1.8)MC(1.2)	0.6	1.8	1.2	4.3	15.9	4.0	75.8

[a]The numbers in parentheses indicate the molar amounts of corresponding metal salts impregnated on the sorbents in mmol/g-sorbent. The amount of $MgCO_3$ in the sorbent SN(0)SC(0)MC(1.2) was 10 wt%, and other sorbents were obtained by loading $NaNO_3$ or Na_2CO_3 onto the sorbent SN(0)SC(0)MC(1.2) prepared

ring to the method described by Zhang et al. [13] Magnesium nitrate solution was prepared by dissolving 15 g of $Mg(NO_3)_2{\cdot}6H_2O$ in 80 ml deionized water along with the preparation of sodium carbonate solution by dissolving 25 g of Na_2CO_3 in 110 ml deionized water. Sodium carbonate solution was gradually added for 2 h using a master flex pump to magnesium nitrate solution with stirring. After the additional stirring for 1 h, the mixed solution was filtered to obtain the wet cake. The wet cake was oven-dried at 120 °C for 12 h. Dried sample was crushed and screened to the particles of 100-120 mesh sizes, and finally activated by the calcination in a muffle furnace at 450 °C for 4 h in air for the CO_2 sorption reaction test.

2. CO_2 Sorption Reaction Tests

CO_2 sorption reaction experiments were conducted using AutoChem II 2920 (Micromeritics). Calcined sorbent particles of about 200 mg were evenly mixed using the same amount of α-Al_2O_3 particles as diluents and loaded onto the quartz fritted tube reactor as a fixed bed of shallow depth. The reactor-loaded fresh sorbents were pretreated using He flow (50 cm^3/min) at 450 °C for 1 h for dehydration, and then the reactor bed temperature was lowered to a set value for the CO_2 sorption reaction. Kinetic data were obtained in the range of 245-310 °C with CO_2 concentrations 2.5, 6.25, 8.75 and 10% at 1 bar using the total reactant gas (CO_2, H_2O and He as a balance) flow rate kept at 80 cm^3/min. Because the experiment at 90 cm^3/min gave no difference in the carbonation conversion behavior from that at 80 cm^3/min, the kinetic experiments were regarded to be conducted without the problem of external mass transfer limitation. To simulate the flue gas holding water vapor, the reactant gas stream was moisturized to contain 10% H_2O. Further details on the kinetic experiments could be found elsewhere [11]. The fractional conversion of MgO on the sorbent was calculated as

$$X = \frac{m_{CO_2}}{m_{MgO}} \quad (2)$$

where, m_{CO_2} and m_{MgO} are the amount of CO_2 reacted and that of MgO of the sorbent in mmoles per gram of sorbents used for the reaction experiments, respectively.

3. Characterization of the Sorbents Prepared

The textural properties of the sorbents were analyzed using N_2 at 77 K in a Micromeritics ASAP 2420. The samples were degassed at 90 °C for 30 min and 200 °C for 4 h prior to each measurement. XRD patterns were obtained using Rigaku Miniflex II desktop X-ray diffractometer with a scan rate of 4°/min using Cu Kα radiation (30 kV, 15 mA). The distribution of metal elements was obtained using the Philips XL-30S FEG scanning electron microscope (SEM) equipped with energy dispersive X-ray spectroscopy (EDS).

RESULTS AND DISCUSSION

1. Advantages of Al_2O_3-supporting

Fig. 2(a) shows the carbonation conversions of the Al_2O_3-supported sorbents in comparison with the unsupported $NaNO_3$-Na_2

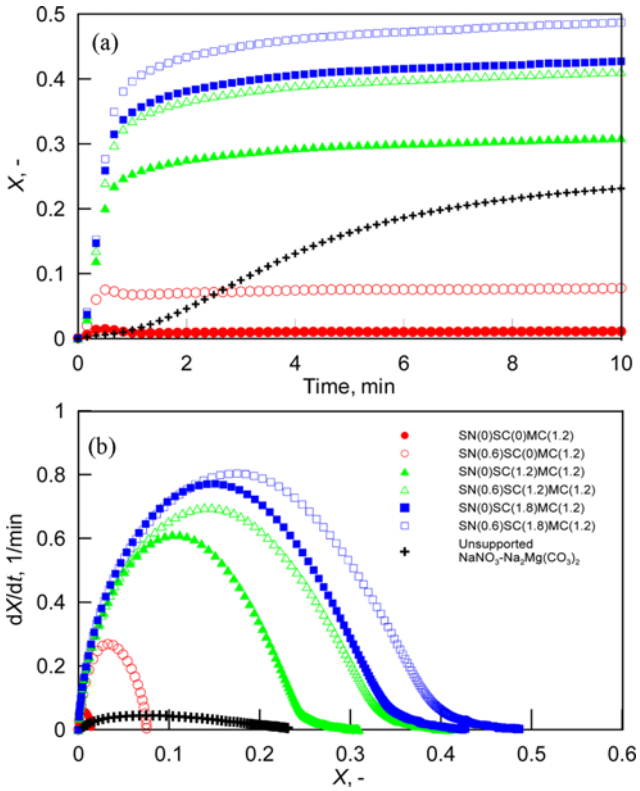

Fig. 2. Carbonation conversions with time (a), and the profiles of carbonation rate changes with the degree of conversion (b) for the Al_2O_3-supported sorbents in comparison with the unsupported $NaNO_3$-$Na_2Mg(CO_3)_2$ sorbent in the sorption reaction at 280 °C, 8.75% CO_2, and 10% H_2O.

$Mg(CO_3)_2$ sorbent in the sorption reaction at 280 °C, 8.75% CO_2, and 10% H_2O, and Fig. 2(b) shows the profiles of carbonation rate changes, obtained by the time-differentiation of the conversion data, with the degree of conversion. As compared with the very slow carbonation conversion over extended time of 10 min for the unsupported sorbent of $NaNO_3$-$Na_2Mg(CO_3)_2$, the Na_2CO_3 and $NaNO_3$-promoted or unpromoted Al_2O_3-supported $MgCO_3$ sorbents show basically rapid conversions as over 80% of their steady state conversions have been early reached within a short reaction time of 1 min. This initial rapid carbonation conversion of the Al_2O_3-supported sorbents would be possibly originating from the increase in the surface-exposed fraction of MgO by being dispersed over the Al_2O_3 support as small clusters. Accordingly, this Al_2O_3-supporting can be an effective way to make MgO sorbents more reactive for the carbonation.

Fig. 3 shows the SEM and EDS mapping images for the Al_2O_3-supported SN(0.6)SC(1.8)MC(1.2) sorbent, indicating that the impregnated magnesium and sodium are well dispersed over the Al_2O_3 support. In accordance with such a good dispersion of Mg and Na compounds on the support, as shown in Fig. 4(a), no XRD patterns attributable to MgO or Na_2CO_3 have been detected for the Al_2O_3-supported SN(0.6)SC(1.8)MC(1.2) sorbent after its calcination. In contrast to this Al_2O_3-supported sorbent, many XRD patterns have been detected for the unsupported $NaNO_3$-$Na_2Mg(CO_3)_2$ sorbent, as shown in Figs. 4(b), 4(c) and 4(d). XRD patterns for eitelite ($Na_2Mg(CO_3)_2$), hydromagnesite ($Mg_5(CO_3)_4(OH)_2{\cdot}4H_2O$) and $NaNO_3$ are detected for this unsupported sorbent at the state as a dried precipitate, as shown in Fig. 4(b). For the sample after calcination, XRD patterns of MgO crystalline phases in high intensities are displayed with those of Na_2CO_3 and $NaNO_3$, as shown in Fig. 4(c). For the sample after the carbonation reaction using 8.75% CO_2 at 280 °C, intensities of the XRD patterns corresponding to MgO phase decrease corresponding to the formation of crystalline phases of $Na_2Mg(CO_3)_2$ as well as $MgCO_3$, as shown in Fig. 4(d). These results indicate that $MgCO_3$ exists, forming large crystalline phases and parts of $MgCO_3$ cannot interact with Na_2CO_3 in the unsupported bulk $NaNO_3$-$Na_2Mg(CO_3)_2$ prepared. As stated by Zhang et al. [13], the difficulty in controlling the amounts of retained Na_2CO_3 and $NaNO_3$ in the synthesis process of the unsupported bulk $NaNO_3$-$Na_2Mg(CO_3)_2$ sorbent via precipitation and filtration can be one of the causes of this poor carbonation reaction activity. Zhang et al. [13] suggested that alternate synthesis methods need to be developed for a reproducible and scalable synthesis. In these regards, the preparation of $NaNO_3$-$Na_2Mg(CO_3)_2$ phase inside pores of a support using the incipient wetness impregnation technique can be a good alternative to the previous method of synthesis via precipitation and filtration. This is particularly advantageous in that controlled amounts of $MgCO_3$, Na_2CO_3 and $NaNO_3$ are retainable inside pores of the support and metal salts impregnated can be induced to be more closely contacted among them to form the phase of $Na_2Mg(CO_3)_2$ by being dispersed in smaller sizes over the support. Although the existence of $Na_2Mg(CO_3)_2$ phase on the Al_2O_3-supported sorbents of this study could not be ascertained by XRD, higher carbonation conversion along with faster kinetics of the supported sorbents containing Na_2CO_3 suggests higher probability of the possible formation of $Na_2Mg(CO_3)_2$ phases on the support.

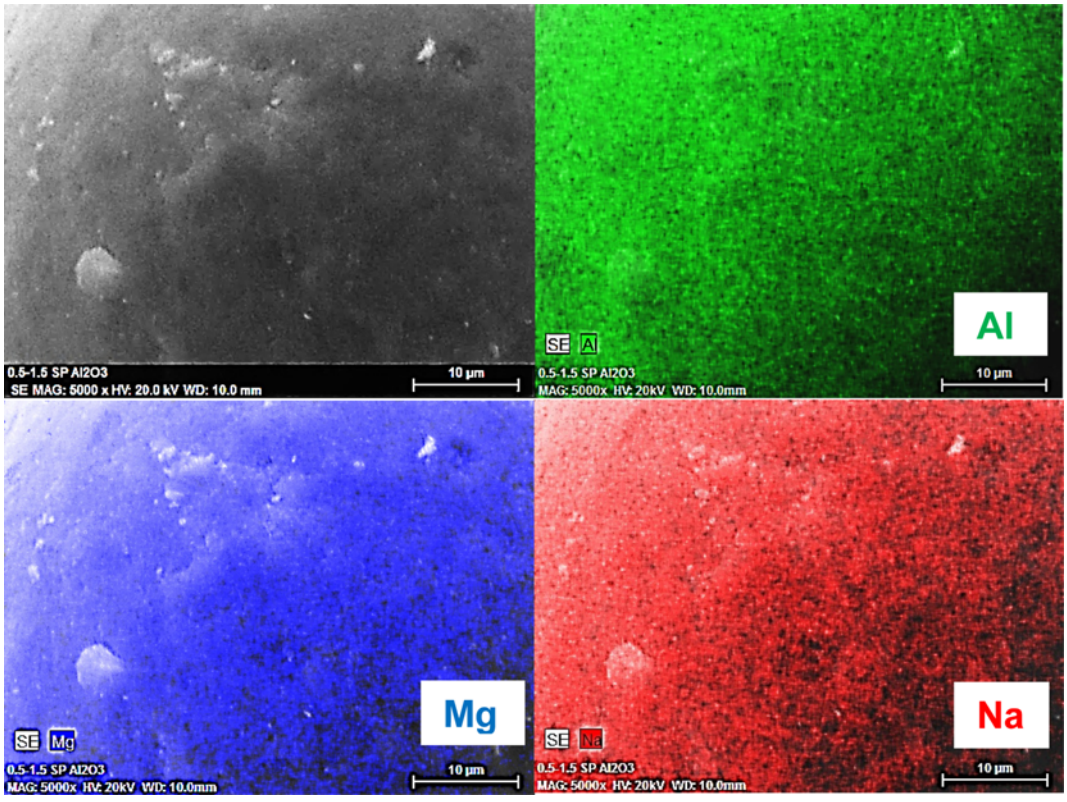

Fig. 3. SEM and EDS mapping images for the Al_2O_3-supported SN(0.6)SC(1.8)MC(1.2) sorbent.

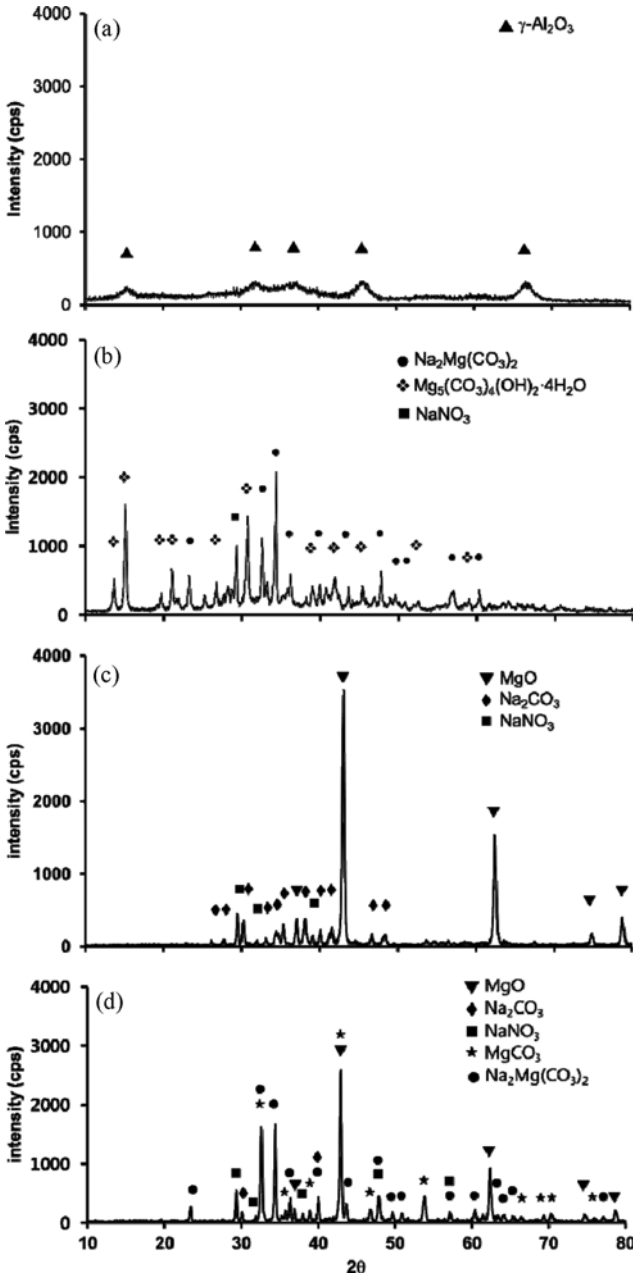

Fig. 4. XRD patterns of the Al_2O_3-supported SN(0.6)SC(1.8)MC(1.2) sorbent after the calcination (a), and the unsupported $NaNO_3$-$Na_2Mg(CO_3)_2$ sorbent at the state as dried precipitate (b), after the calcination (c), and after the carbonation reaction (d).

2. Promotion by the $NaNO_3$ and/or Na_2CO_3 Addition to Mg CO_3/Al_2O_3

As shown in Fig. 2(a), the unpromoted $MgCO_3/Al_2O_3$ sorbent has a negligible reactivity for the carbonation reaction showing only a small conversion of MgO, about 1.3% in the reaction for 10 min at 280 °C and 8.75% CO_2. However, this low reactivity of $MgCO_3/Al_2O_3$ has been greatly improved when promoted with Na_2CO_3 and/or $NaNO_3$. The addition of Na_2CO_3 to the $MgCO_3/Al_2O_3$ in an equal molar amount to $MgCO_3$ brings about a big promotion in the carbonation reactivity of MgO, and the more Na_2CO_3 was added, the more carbonation conversion was achieved. Also, the addition of $NaNO_3$ to the $MgCO_3/Al_2O_3$ or to the Na_2CO_3-$MgCO_3/Al_2O_3$ in a half molar amount to $MgCO_3$ leads to the increase of carbonation conversion.

For the Na_2CO_3-promoted sorbents, the promotion is probably achieved by forming the phase of $Na_2Mg(CO_3)_2$ as discussed above. On the possible way of the promotion by $NaNO_3$-addition, Zhang et al. [13] suggested that $NaNO_3$ penetrates the product double salt grain boundaries with its high wetting property over many oxides and metal surfaces, and provides a liquid channel for a fast CO_2 diffusion during the reaction. In view of the melting point of pure $NaNO_3$ around 306-308 °C [13,15], melted $NaNO_3$ can spread out instantly and cover the surface of $MgCO_3/Al_2O_3$ or Na_2CO_3-$MgCO_3/Al_2O_3$ during the sample calcination at 450 °C taken for the conversion of $MgCO_3$ to MgO prior to the sorption reaction. It also needs to be mentioned for the sample calcination that a reversible thermal dissociation reaction of melted $NaNO_3$ can occur at 450 °C as follows [15]:

$$NaNO_3(l) \leftrightarrow NaNO_2(l) + \frac{1}{2}O_2(g), \quad (3)$$

For the resulting $NaNO_3/NaNO_2$ mixture ranging from 0.25 to 0.80 in mole fraction of $NaNO_2$, Berg et al. [15] reported a solidus at 230 °C and liquidus transition at 235-282 °C. In this respect, the reaction temperature 280 °C for data shown in Fig. 2 can be regarded enough for the resulting mixture of $NaNO_3/NaNO_2$ to be partly melted. Therefore, Zhang et al's [13] proposal for the fast CO_2 diffusion through a liquid channel would be a possible working route for the promoted carbonation conversion of MgO in our study.

3. Kinetic Evaluation of the Promotional Effects of $NaNO_3$ and/or Na_2CO_3

For all these Al_2O_3-supported $MgCO_3$-based sorbents, it is characteristic that starting rates of the carbonation conversion appear to be near zero, as shown in Fig. 2(b). As a result of this incipient retardation of the carbonation reaction, the carbonation conversion curves in Fig. 2(a) appear more or less sigmoid. Although the conversion data here were obtained by measuring the CO_2 concentration in the reactant gas coming through a shallow fixed bed of the sorbents, it can be thought that this sigmoid conversion behavior was not attributed to the measurement artifacts in view of some papers reporting the same behavior from the experiments using TGA. Monazam et al. [12] reported sigmoid conversion curves in the CO_2 sorption experiments for the silica-grafted amine sorbent using TGA, by which the amount of CO_2 uptake in the sorbent carbonation reaction could be directly measured. They explained that the sigmoid conversion behavior of the sorbent carbonation is attributable to the carbonation process of first nucleation and then crystalline growth, and that an induction period is required before the nucleation. For the carbonation of unsupported K_2CO_3 or Al_2O_3-supported K_2CO_3 sorbents using TGA, Zhao et al. [17,18] also reported the same sigmoid conversion behavior. Therefore, such observed sigmoid conversion behavior in the very initial reaction period might be a common intrinsic phenomenon in a heterogeneous carbonation reaction between gas phase CO_2 and solid phase sorbents.

In the CO_2 sorption reaction using solid sorbents, as a gas-solid

heterogeneous reaction, kinetic rate of the carbonation conversion is generally influenced by three factors such as sorption reaction temperature, degree of carbonation conversion of the sorbent, and gas phase concentrations of CO_2, as described in Lee at al. [11]

$$r=k\cdot f(X)\cdot f(y_{CO_2}) \quad (4)$$

where, k is a reaction rate constant with Arrhenius temperature dependency, f(X) is a rate-affecting term as a function of the fractional carbonation conversion, X, of the sorbent, and $f(y_{CO_2})$ is a rate dependency as a function of CO_2 mole fraction, y_{CO_2}, in the gas phase. To evaluate quantitatively the effect of the promoters on the carbonation reaction rate here, a model capable of describing the sigmoid conversion behavior is required, and such a carbonation conversion model as developed for K_2CO_3/ZrO_2 sorbent [11] is employed here as follows:

$$X=X_u\left\{1-\exp\left(-\frac{at^b}{X_u}\right)\right\} \quad (5)$$

where, X_u is an ultimate fractional carbonation conversion appearing as a steady state value, and a and b are parameters to determine the overall shape of a time dependent conversion curve. For a reaction at a constant CO_2 concentration, the carbonation conversion rate can be obtained by differentiating Eq. (5) as follows:

$$\frac{dX}{dt}=k'\cdot f(X) \quad (6)$$

where,

$$k'=b\,a^{\frac{1}{b}}X_u^{1-\frac{1}{b}} \quad (7)$$

$$f(X)=\left\{-\ln\left(1-\frac{X}{X_u}\right)\right\}^{1-\frac{1}{b}}\left(1-\frac{X}{X_u}\right) \quad (8)$$

In Eq. (6), k' can be regarded as a tentative kinetic rate constant. Values of the parameters can be determined by least square curve fitting of the conversion data to Eq. (5). Fig. 5(a) shows a typical result of such a least square fit of the sigmoid conversion data within 1 min for the Al_2O_3-supported sorbent of SN(0.6)SC(1.2)MC(1.2) to determine the kinetic parameters, X_u=0.332, b=2.154, a=1.870, and k'=1.594 min^{-1} with the regression coefficient of 0.999. Fig. 5(b) shows the comparison of the rate of conversion between experimental and predicted using Eq. (6) with the above-determined parameter values. In this kinetic analysis, the conversion data within 1 min are used instead of 10 min, as shown in Fig. 2(a), because most of the carbonation conversions have been achieved within initial 1 min and the kinetic information within this short contact time is crucial to the determination of the sorbent applicability to a riser-type fast fluidized bed. Such determined values of X_u and k' for the sorbents prepared here are summarized in Table 2.

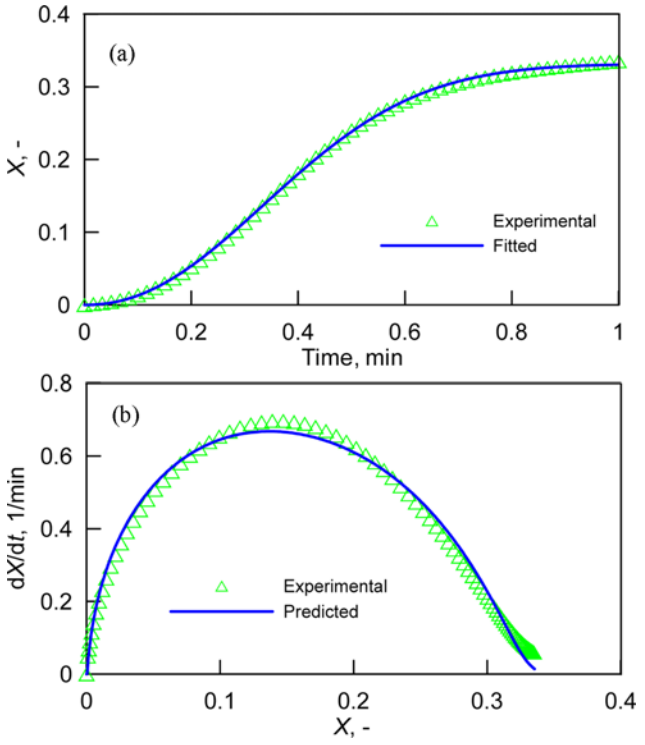

Fig. 5. Least squares fit to Eq. (5) of the conversion data within 1 min to determine the kinetic parameters: X_u=0.332, b=2.154, a=1.870, and k'=1.594 min^{-1} (a), and comparison of the rate of conversion between experimental and predicted using Eq. (6) with the above determined parameter values (b), for the Al_2O_3-supported sorbent of SN(0.6)SC(1.2)MC(1.2) experimented at 280 °C, 8.75% CO_2 and 10% H_2O.

Relative to the SN(0)SC(0)MC(1.2), SN(0.6)SC(1.8)MC(1.2) shows

Table 2. CO_2 sorption kinetic parameters determined for Al_2O_3-supported $MgCO_3$-based sorbents using the conversion data within 1 min at 280 °C, 8.75% CO_2, and 10% H_2O

Sorbents	X_u	k', min^{-1}	R^2	Relative k'				
SN(0)SC(0)MC(1.2)	0.013	0.202	0.946	1				
SN(0)SC(1.2)MC(1.2)	0.250	1.392	0.991	6.9		1	1	
SN(0)SC(1.8)MC(1.2)	0.343	1.764	0.990	8.8		1.3		1
SN(0.6)SC(0)MC(1.2)	0.071	0.720	0.990	3.6	1			
SN(0.6)SC(1.2)MC(1.2)	0.332	1.594	0.999	7.9	2.2	1	1.2	
SN(0.6)SC(1.8)MC(1.2)	0.392	1.860	0.997	9.2	2.6	1.2		1.1
Unsupported $NaNO_3$-$Na_2Mg(CO_3)_2$[a]	0.231	0.092	0.994					

[a]Kinetic data of this unsupported sorbent were determined using conversion data for 10 min

9.2-times higher kinetic rate for the carbonation reaction, as listed in Table 2. This large promotion in the kinetic rate of the SN(0.6)SC(1.8)MC(1.2) seems to be mostly attributed to the addition of Na_2CO_3 to $MgCO_3/Al_2O_3$ in view of the 8.8 times higher kinetic rate of SN(0)SC(1.8)MC(1.2) relative to SN(0)SC(0)MC(1.2). As compared to this large kinetic effect of the Na_2CO_3 addition, the effect of $NaNO_3$ addition to the SN(0)SC(0)MC(1.2) is limited to giving the 3.6-times higher kinetic rate at its best. From this kinetic evaluation, it can be inferred that Na_2CO_3 could make a big promotion by being directly involved in such structural modification of the supported $MgCO_3$ as forming the double salt phase $Na_2Mg(CO_3)_2$, but $NaNO_3$ promotion is limited to a relatively small magnitude by its subsidiary role of just providing a liquid channel for fast diffusion of CO_2, as discussed above.

Table 3. Parameter values determined in the least squares fit of conversion data to Eq. (5) for the Al_2O_3-supported SN(0.6)SC(1.8)MC(1.2) sorbent

T, K	y_{CO_2}, -	X_u, -	b, -	a, min^{-b}	k′, min^{-1}	R^2
518	0.1	0.432	2.199	3.183	2.354	0.997
533	0.1	0.425	2.380	3.003	2.301	0.999
553	0.1	0.389	2.232	2.813	2.107	0.998
573	0.1	0.371	2.166	2.617	1.980	0.999
553	0.025	0.330	2.382	0.610	1.016	0.999
553	0.0625	0.355	2.273	2.168	1.787	0.999
553	0.0875	0.392	2.178	2.132	1.860	0.999

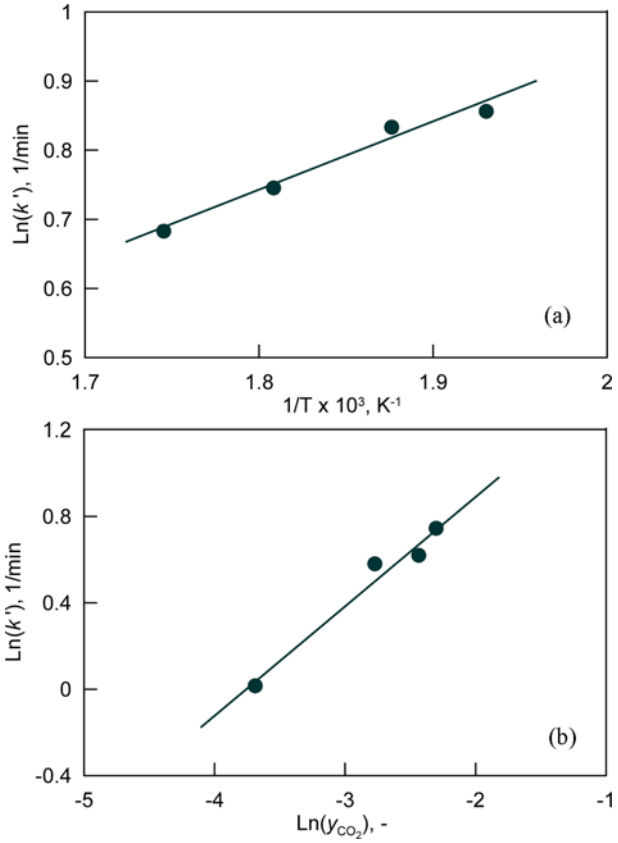

Fig. 6. Rate constant k′ dependency on the sorption reaction temperature (a) and the gas phase mole fraction of CO_2 (b) for the Al_2O_3-supported SN(0.6)SC(1.8)MC(1.2).

4. Carbonation Reaction Kinetics of the SN(0.6)SC(1.8)MC(1.2) Sorbent

Because the Al_2O_3-supported SN(0.6)SC(1.8)MC(1.2) sorbent shows the best reaction performance, its kinetic equation needs to be established. Table 3 lists values of the parameters determined by least square curve fitting of the conversion data within 1 min to Eq. (5) for the SN(0.6)SC(1.8)MC(1.2) sorbent at different reaction temperatures and gas phase mole fractions of CO_2. Fig. 6(a) shows the Arrhenius plot of in the carbonation reaction over SN(0.6)SC(1.8)MC(1.2). The values of apparent activation energy and pre-exponential factor were determined as $E_{A,app}$=−8.161 kJ·mol^{-1} and A=0.358 min^{-1}, respectively. The negative apparent activation energy obtained here indicates that the adsorption of CO_2 onto the sorbent is involved in the carbonation reaction process as a rate-determining step with concurrent release of the heat of adsorption [11]. Consequently,

$$k' = 0.358\exp\left(\frac{8161}{RT}\right) \tag{9}$$

where, R is the gas constant.

Here, if the sorption rate dependency on the CO_2 concentration in Eq. (2) follows *n*-th power law,

$$f(y_{CO_2}) = k'' \cdot y_{CO_2}^n \tag{10}$$

where, k″ is a constant introduced for the value of $f(y_{CO_2})$ that needs to be adjusted to become unity at a specified set of reaction condition of temperature and gas phase mole fraction of CO_2. Using Eqs. (8) and (10), Eq. (4) can be finally expressed as follows:

$$r = \frac{dX}{dt} = k \cdot \left\{-\ln\left(1-\frac{X}{X_u}\right)\right\}^{1-\frac{1}{b}}\left(1-\frac{X}{X_u}\right)\cdot y_{CO_2}^n \tag{11}$$

where, k is the reaction rate constant obtained as follows:

$$k = k'' \cdot k' \tag{12}$$

Fig. 6(b) shows the kinetic rate dependence on the gas phase mole fractions of CO_2 for data at 553 K, to determine the reaction order. The data are well represented by a straight line with a slope as the reaction order, n=0.51. In Eq. (10), the value of the constant k″ is so determined that $f(y_{CO_2})$ could become unity at y_{CO_2}=0.1 and T=553 K, resulting in k″=3.236. Eq. (10) becomes

$$f(y_{CO_2}) = 3.236 y_{CO_2}^{0.51} \tag{13}$$

Therefore, the reaction rate constant k in Eq. (12) is finally expressed as follows:

Table 4. Linear correlation equations for the model parameters with T (K) and CO_2 mole fraction, y_{CO2}

Correlation equations	R^2	
X_u=0.97−0.0012T+0.886y_{CO_2}	0.971	(15)
b=2.258	-	
a=6.019-0.0107T+27.01y_{CO_2}	0.962	(16)

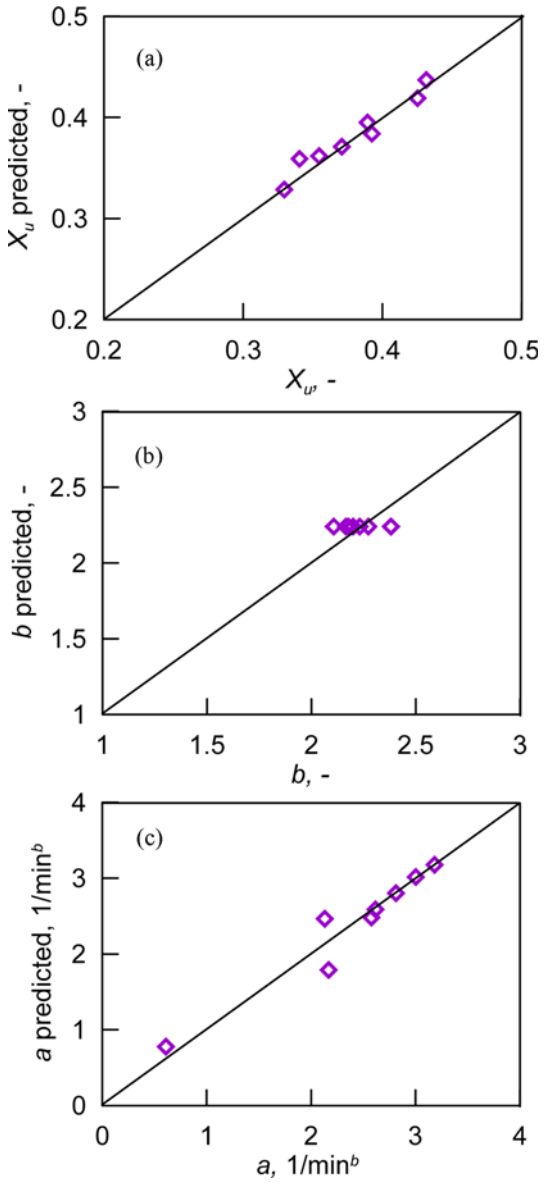

Fig. 7. Parity plots for the kinetic parameters, X_u (a), b (b), and a (c), between the values predicted using the correlation equations listed in Table 4 and those given in Table 3.

$$k = 1.158\exp\left(\frac{8161}{RT}\right) \quad (14)$$

Because the parameter values of X_u, b and a listed in Table 3 are varied depending on the reaction temperature and the gas phase mole fraction of CO_2, there is a need to correlate them with the two reaction variables. The results of the linear correlation analysis are listed in Table 4. Fig. 7 shows the parity plots for the correlation results. The parameters X_u and a were well correlated with T and y_{CO_2} by Eqs. (15) and (16) in Table 4, respectively, but, for b varying within a narrow range, an average value 2.258 was taken because the correlation was not successful.

Fig. 8 shows the comparison of the carbonation rate change with the degree of sorbent conversion between experimental and predicted by Eq. (11), where the parameter values have been obtained

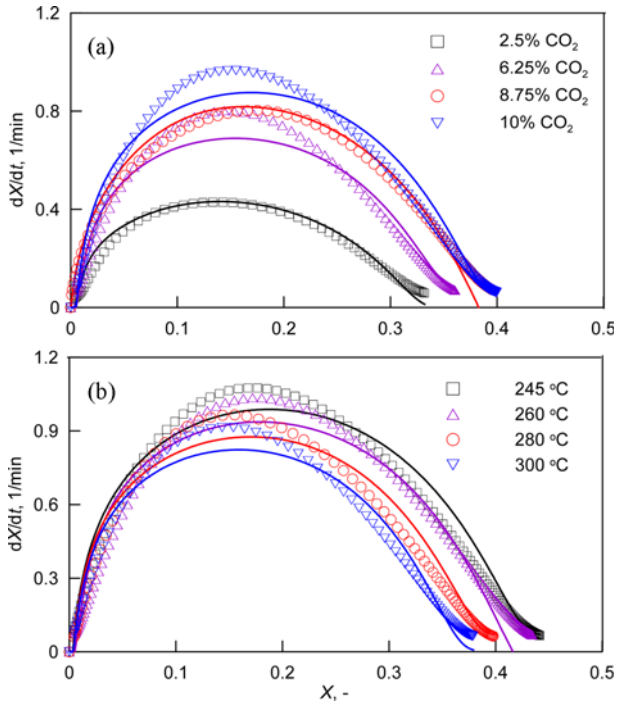

Fig. 8. Comparison of the carbonation rate change with the degree of conversion between experimental and predicted (shown as lines) by Eq. (11) for data experimented with different CO_2 concentrations at 280 °C (a) and with different temperatures at 10% CO_2 (b) for the Al_2O_3-supported SN(0.6)SC(1.8)MC(1.2).

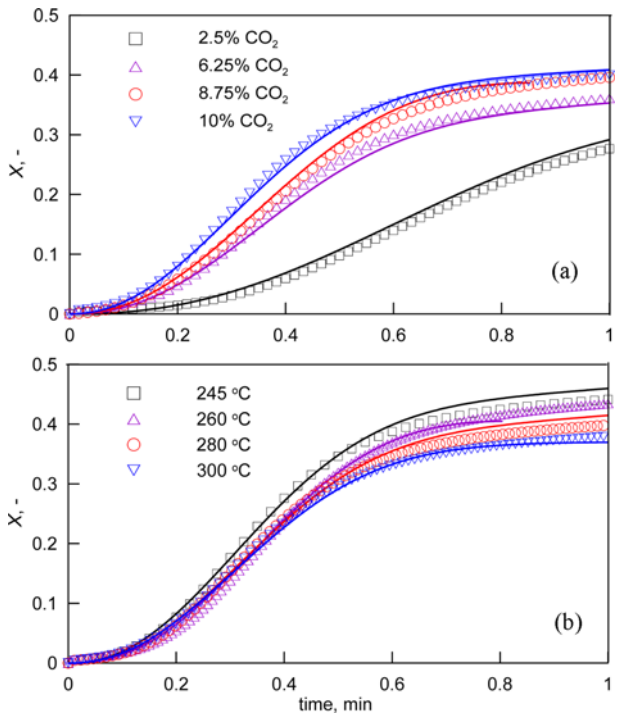

Fig. 9. Comparison between experimental conversions and the kinetic model predictions (shown as lines) obtained by integrating Eq. (11) for data experimented with different CO_2 concentrations at 280 °C (a) and with different temperatures at 10% CO_2 (b) for the Al_2O_3-supported SN(0.6)SC(1.8)MC (1.2).

using the correlation equations listed in Table 4. The kinetic model predictions are shown to be satisfactory in depicting the experimental rate data on the whole, although some underestimations are made for data at maximal rates. Fig. 9 shows the comparison between the experimental sorbent conversions and the kinetic model predictions obtained by integrating Eq. (11). In view of excellent agreement between experimental and calculated results at different reaction temperatures and gas phase CO_2 concentrations, the kinetic model developed here is capable of providing a fine prediction for the SN (0.6)SC(1.8)MC(1.2) sorbent conversion in the range of 245-300 °C with CO_2 concentrations 2.5-10% at 1 bar under 10% moisture condition. Although not presented in Fig. 8, experimental data at 310 °C are not well predicted by the kinetic model. This is attributed to the shift of thermodynamic equilibrium toward the decarbonation reaction of $Na_2Mg(CO_3)_2$, according to Zhang et al. [13], which is favored at higher temperatures from about 310 °C.

5. Evaluation of the SN(0.6)SC(1.8)MC(1.2) Sorbent Applicability to a Riser-type Carbonator

Based on its kinetics obtained above, the sorbent SN(0.6)SC(1.8)MC(1.2) needs to be examined with respect to its applicability to a riser-type carbonator through a simple model assuming the average retention time (t_s) of solid sorbents in the riser. In view of the kinetic equation obtained and the profiles of the carbonation rate change with the conversion as shown in Fig. 8, the carbonation rate in the riser tube can be configured as follows. In the region very near to the riser entrance, the rate could be accelerated by the high concentration of CO_2 of incoming flue gas, but limited by the initial rate retardation occurring on the incoming sorbents of near zero degree of carbonation due to their possible total decarbonation in the regenerator. In the region near to the riser exit, including the rate limitation by the lowered concentration of CO_2, the rate can be severely limited by the degree of the carbonation conversion achieved if it is close to the X_u. If the carbonation conversion of the sorbent at the riser exit is controlled to be kept around the optimum at which the maximum carbonation rate (r_m) is attained, the rate dependence on the degree of the conversion would disappear. As shown in Fig. 8(a), because r_m varies with the CO_2 concentration, the lowest CO_2 concentration of the flue gas at the riser

Table 5. Estimation of the riser carbonator performance in the CO_2 capture using the SN(0.6)SC(1.8)MC(1.2) sorbent[a]

		Case I	Case II	Case III
U_o, superficial gas velocity	[m/s]	1	1.5	2
t_s, sorbent retention time assumed	[s]	47.20	22.91	13.86
r_m, max carbonation rate	[1/min]	0.357	0.357	0.357
X_e, carbonation conversion achieved	[mol-CO_2/mol-Mg]	0.28	0.14	0.08
λ, CO_2 uptake per m^3-sorbent ($=22.4\times10^{-3}L_{Mg}X_e\rho_s$)	[m^3-CO_2/m^3-Sb]	7.14	3.47	2.10
γ_s, required volume of sorbent for treating 1 m^3 flue gas ($=135/\lambda$)	[L-Sb/m^3-gas]	18.90	38.95	64.38
δ_s, volume fraction of sorbents in the riser ($=\gamma_s/(1000+\gamma_s)$)	[m^3-Sb/m^3-reactor]	0.019	0.037	0.060
ε, voidage in the riser ($=1-\delta_s$))	[m^3-gas/m^3-reactor]	0.981	0.963	0.940
Q_o, feeding rate of flue gas ($=3600U_oA$)	[m^3-gas/h]	13.97	20.95	27.93
W_s, required sorbent circulation rate ($=Q_o\rho_s/3600$)	[kg-Sb/s]	0.069	0.214	0.473
G_s, sorbent mass flux in the riser ($=W_s/A$)	[kg-Sb/m^2/s]	17.88	55.27	121.80
Fr, Froude number ($=U_o/\sqrt{gD}$)	[-]	1.21	1.81	2.41
φ, slip factor	[-]	6.01	4.46	3.69
U_s, average velocity of sorbent particles ($=U_o/\varepsilon\varphi$)	[m/s]	0.17	0.35	0.58
t_s, calculated ($=H/U_s$)	[s]	47.20	22.91	13.86

[a]Conditions and data for the calculation

1) Flue gas composition: 15% CO_2, 10% H_2O, 75% N_2
2) CO_2 removal from the flue gas throughout the riser: 90%
3) CO_2 composition of the riser exit flue gas: 1.73%
4) Riser temperature and pressure: 280 °C, 1 atm
5) Loading amount of Mg per kg-sorbent: L_{Mg}=1.2 mol-Mg/kg-Sb
6) Volume of CO_2 removed from 1 m^3 of the flue gas: 135 L/m^3-gas
7) Density of flue gas feed at 280 °C, 1 atm using the ideal gas law: ρ_g=0.648 kg/m^3
8) Bulk density and diameter of sorbent particle: ρ_s=946 kg/m^3, d_s=100 μm
9) Molar average viscosity of the flue gas at 280 °C, 1 atm: $\mu=2.7\times10^{-5}$ Pa·s data by Geankoplis [20]: $\mu_{CO_2}=2.5\times10^{-5}$ Pa·s, $\mu_{H_2O}=1.92\times10^{-5}$ Pa·s, $\mu_{H_2}=2.84\times10^{-5}$ Pa·s, $\mu=0.15\mu_{CO_2}+0.1\mu_{H_2O}+0.75\mu_{N_2}$
10) Terminal particle velocity at the flue gas of 280 °C, 1 atm: U_t=0.444 m/s by Kunii and Levenspiel [21]:

$$U_t=\left[\frac{4}{225}\frac{(\rho_s-\rho_g)^2g^2}{\rho_g\mu}\right]^{1/3}d_s,\quad \text{for } 0.4<Re_p=\frac{d_s\rho_gU_t}{\mu}<500$$

11) Froude number at terminal particle velocity: $Fr_t=U_t/\sqrt{gD}=0.534$
12) Inside diameter, height and cross-sectional area of the riser tube: D=0.0703 m, H=8 m, $A=3.88\times10^{-3}$ m^2

exit determines the slowest r_m along the riser tube. For the riser model calculation here, the following assumptions are made: (1) the rate of sorbent carbonation throughout the riser tube follows the slowest r_m; (2) steady-state plug-flow of gas and sorbent through a cylindrical riser; (3) constant volume fraction of sorbents along the height of the riser; and (4) isothermal operation at 553 K.

Under these assumptions, t_s in the riser is initially assumed for a given value of superficial flue gas velocity (U_o), as listed in Table 5. Under the condition that the CO_2 composition of the flue gas feed is 15% and the recovery of CO_2 from the flue gas throughout the riser is 90%, the concentration of CO_2 in the riser exit gas is the lowest as 1.73%. For this exit gas of y_{CO_2}=0.0173 at 553 K, Eqs. (14) and (15) give k=6.84 min^{-1} and X_u=0.322. Then, the carbonation rate of the sorbent with the degree of the conversion can be obtained using Eq. (11) like the profile shown in Fig. 8(a). For the riser-exit flue gas of y_{CO_2}=0.0173 at 553 K, the carbonation rate is maximized at X=0.12, giving r_m=0.357 min^{-1}. Once the carbonation conversion achieved (X_e) throughout the riser is calculated by $X_e=r_m t_s/60$, CO_2 uptake (λ) of the sorbent can be determined. This enables us to calculate, for 1 m^3 of the flue gas fed, the required volume of the sorbent (γ_s) to capture 90% of CO_2 and the void fraction (ε) of the riser, as listed in Table 5. Multiplying U_o by the cross-sectional area (A) of the riser gives the feeding rate of the flue gas (Q_o). Then, the sorbent circulation rate (W_s) required for treating Q_o can be calculated, and the sorbent mass flux (G_s) as well. Slip factor (φ) defined as a relative gas velocity to the average velocity (U_s) of sorbent particles in the riser can be calculated using the correlation by Patience et al. [19] as follows:

$$\varphi \equiv \frac{U_o}{\varepsilon U_s} = 1 + \frac{5.6}{Fr} + 0.47 Fr_t^{0.41} \quad (17)$$

where, Fr and Fr_t are the Froude numbers at the superficial gas (U_o) and terminal particle (U_t) velocities, respectively. As listed in Table 5, Patience et al's correlation gives φ values of 6.01, 4.46, and 3.69 for given U_o values of 1, 1.5, and 2 m/s. For these φ values, U_s estimated by Eq. (17) are 0.17, 0.35, and 0.58 m/s. In such cases, the calculated values of t_s in the riser are exactly same as those of initial assumption, 47.2, 22.91, and 13.86 s, respectively.

Results of this model calculation suggest that the sorbent SN(0.6)SC(1.8)MC(1.2) has enough kinetic rate at 553 K to be applied to the riser carbonator of D=0.0703 m and H=8 m for the removal of 90% of CO_2 in the flue gas fed. Note that this simple model only serves as a preliminary tool for investigating the possibility of the sorbent SN(0.6)SC(1.8)MC(1.2) characterized with the kinetics obtained above in the application to a riser sorber where the contact time between the sorbent and the flue gas is limited in the range of 10-60 s. Case II in Table 5 is estimated to be the best option in view of the sorbent retention time (t_s=22.91 s) and the carbonation conversion achieved (X_e=0.14). In case I with t_s=47.2 s, the carbonation conversion achieved in the riser is too high as 0.28, passing over the conversion X=0.12 where the maximum rate is attained. Resultantly, the carbonation rate in the later part of the riser would be limited. This leads to an insufficient use of the riser reactor in its capacity of the flue gas treatment. In case III with t_s=13.86 s, the carbonation conversion achieved as low as 0.08 could be a limiting factor for the carbonation rate throughout the whole riser, leading to the problem of an inefficient use of the sorbent. In case II with t_s=22.91 s, the carbonation conversion achieved is 0.14, which is a little higher than the conversion X=0.12 where the maximum carbonation rate is attained. Because Eq. (11) gives r=0.354 min^{-1}, when X=0.14 and y_{CO_2}=0.0173, the carbonation reaction rate at this degree of carbonation conversion achieved is nearly the same as the maximum rate, r_m=0.357 min^{-1}. Accordingly, assumption (1) made above for the model becomes satisfied with this result in the carbonation rate. The carbonation reaction in case II could therefore proceed at a rate close to the maximum rate, leading to a highly efficient use of the sorbent from the viewpoint of its kinetic characteristics, by which the riser reactor could be almost fully utilized in terms of its capacity of the flue gas treatment.

CONCLUSIONS

For CO_2 capture from flue gas, the Al_2O_3-supported $MgCO_3$ (1.2 mmol/g) promoted with $NaNO_3$ (0.6 mmol/g) and Na_2CO_3 (1.8 mmol/g), noted as SN(0.6)SC(1.8)MC(1.2), prepared by incipient wetness pore volume impregnation, was evaluated as a promising sorbent at intermediate temperatures of 240-300 °C due to its facilitated kinetics, enough to be applicable to a riser-type fast fluidized bed reactor with a short retention time of sorbent particles less than 1 min. Kinetics improvement of the sorbent was thought to be basically contributed by the effect of Al_2O_3-supporting, increasing the fraction of surface-exposed $MgCO_3$ by being dispersed on the porous support surface. As for the effect of the salts added to $MgCO_3/Al_2O_3$, the improvement resulted primarily from the direct involvement of Na_2CO_3 in the structural modification of the supported $MgCO_3$ by forming the double salt phase $Na_2Mg(CO_3)_2$, and secondarily, from the role of $NaNO_3$ providing a liquid channel for fast diffusion of CO_2. The sorption kinetics of the sorbent SN(0.6)SC(1.8)MC(1.2) showing the best performance was derived as follows using conversion data within 1 min in the range of T=510-573 K and y_{CO_2}=0.025-0.1: $r\left(\frac{1}{min}\right) = k \cdot \left\{-\ln\left(1-\frac{X}{X_u}\right)\right\}^{1-\frac{1}{b}} \left(1-\frac{X}{X_u}\right) \cdot y_{CO_2}^n$ where, the reaction rate constant, $k\left(\frac{1}{min}\right)=1.158\exp\left(\frac{8161}{RT}\right)$; the parameter, b=2.258; the ultimate carbonation conversion of MgO, X_u=0.97−0.0012T+0.886 y_{CO_2}; the reaction order with respect to the gas phase mole fraction of CO_2, n=0.51.

ACKNOWLEDGEMENTS

This work is supported by Korea Carbon Capture & Sequestration R&D center (NRF-2011-0031976). It is thankfully acknowledged that D. K. Lee participated in this work during his one year sabbatical stay at KRICT under the financial support from this project as well as from Gwangju University.

NOMENCLATURE

a : kinetic parameter in Eq. (5) [$1/min^b$]
b : kinetic parameter in Eq. (5) [-]
k : reaction rate constant [1/min]

k' : tentative reaction rate constant [1/min]
k'' : constant in Eq. (10) [-]
m_{CO_2} : amount of CO_2 captured by sorbent [mmol-CO_2/g-sorbent]
m_{MgO} : amount of MgO loaded onto the sorbent [mmol-MgO/g-sorbent]
n : reaction order with respect to y_{CO_2} [-]
R : gas constant, 8.314 [J/mol/K]
r : rate of the sorbent carbonation conversion [1/min]
T : temperature [K]
t : time [min]
y_{CO_2} : mole fraction of CO_2 in the gas phase [-]
X : fractional carbonation conversion of MgO [-]
X_u : ultimate carbonation conversion of MgO [-]

REFERENCES

1. A. Samanta, A. Zhao, G. K. H. Shimizu, P. Sarkar and R. Gupta, *Ind. Eng. Chem.* Res., **51**, 1438 (2012).
2. M. Zaman and J. H. Lee, *Korean J. Chem. Eng.*, **30**, 1497 (2013).
3. H. Hayashi, J. Taniuchi, N. Furuyashiki, S. Sugiyama, S. Hirano, N. Shigemoto and T. Nonaka, *Ind. Eng. Chem. Res.*, **37**, 185 (1998).
4. J. C. Abanades, E. J. Anthony, D. Y. Lu, C. Salvador and D. Alvarez, *AIChE J.*, **50**, 1614 (2004).
5. C.-H. Yu, C.-H. Huang and C.-S. Tan, *Aerosol Air Quality Res.*, **12**, 745 (2012).
6. K. Kim, D. Kim, Y.-K. Park and K. S. Lee, *Int. J. Greenhous Gas Control*, **26**, 135 (2014).
7. M. Iijima, T. Nagayasu, T. Kamijyo and S. Nakatani, *Mitsubishi Heavy Industries Technical Review*, **48**, 26 (2011).
8. C.-K. Yi, S.-H. Jo, Y. Seo, J.-B. Lee and C.-K. Ryu, *Int. J. Greenhouse Gas Control*, **1**, 31 (2007).
9. J.-H. Choi, C.-K. Yi and S.-H. Jo, *Korean J. Chem. Eng.*, **28**, 1144 (2011).
10. R. Veneman, Z. S. Li, J. A. Hogendoorn, S. R. A. Kersten and D. W. F. Brilman, *Chem. Eng. J.*, **207-208**, 18 (2012).
11. D. K. Lee, D. Y. Min, H. Seo, N. Y. Kang, W. C. Choi and Y. K. Park, *Ind. Eng. Chem. Res.*, **52**, 9323 (2013).
12. E. R. Monazam, L. J. Shadle, D. C. Miller, H. W. Pennline, D. J. Fauth, J. S. Hoffman and M. L. Gray, *AIChE J.*, **59**, 923 (2013).
13. K. Zhang, X. S. Li, Y. Duan, D. L. King, P. Singh and L. Li, *Int. J. Greenhouse Gas Control*, **12**, 351 (2013).
14. S. G. Mayorga, S. J. Weigel, T. R. Gaffney and J. R. Brzozowski, US Patent, 6,280,503 B1 (2001).
15. T. Bauer, D. Laing, U. Kröner and R. Tamme, *Int. J. Thermophys.*, **33**, 91 (2012).
16. R. W. Berg, D. H. Kerridge and P. H. Larsen, *J. Chem. Eng. Data*, **51**, 34 (2006).
17. C. Zhao, X. Chen and C. Zhao, *Ind. Eng. Chem. Res.*, **51**, 14361 (2012).
18. C. Zhao, X. Chen and C. Zhao, *Energy Fuels*, **26**, 1401 (2012).
19. G. S. Patience, J. Chaouki, F. Berruti and S. R. Wong, *Powder Technol.*, **72**, 31 (1992).
20. C. J. Geankoplis, *Transport processes and separation process principles*, 4th Ed., Prentice Hall, U.S.A. (2003).
21. D. Kunii and O. Levenspiel, *Fluidization Engineering*, Wiley, N.Y. (1969).